PHYSICAL REVIEW B VOLUME 18, NUMBER 12 15 DECEMBER 1978

Chemisorption of oxygen atoms on aluminum (111): A molecular-orbital cluster study

D. R. Salahub and M. Roche
Département de Chimie, Université de Montréal, Montréal, Québec, Canada H3C 3V1

R. P. Messmer
General Electric Company, Corporate Research and Development, Schenectady, New York 12301

(Received 16 August 1978)

Self-consistent-field $X\alpha$ scattered-wave molecular-orbital calculations have been performed for clusters containing up to 22 aluminum atoms representing the (111) surface of aluminum in interaction with an oxygen atom at various positions above, in, and below the surface. Reasonable agreement with experimental photoemission results for the valence and Al-2p core regions of the spectrum was obtained for two distinct positions of the oxygen atom. The first of these has the oxygen atom between 1 and 2 bohrs above an unrelaxed surface, while the second has the oxygen atom in the first surface layer which has been relaxed by enlarging the threefold site. Both of these models are consistent with available experimental data for some coverage between zero and one monolayer. Additional, as yet unobserved, oxygen-related structure is predicted in the valence region between -5 eV and the Fermi level similar to our previous predictions for Al(100) + O, which have subsequently been born out experimentally.

I. INTRODUCTION

This paper is concerned with the chemisorption of oxygen atoms on the (111) surface of aluminum and is a sequel to our previous work on the (100) surface.[1-3] In order to save space, the reader is referred to these earlier papers for the majority of the historical background and a discussion of the conceptual framework and technical implementation of the molecular-cluster approach to the surface problems. In Sec. I we will limit ourselves to bringing the bibliography up to date, as some important experiments have been performed since our previous papers, and to a brief description of the success of our approach for the chemisorption of oxygen on Al(100) so as to put our new results for the (111) surface in proper perspective.

With respect to this latter point, our previous calculations indicated that, at the level of resolution currently obtained in photoemission experiments, three oxygen-related features should be present in the density of states for the initial stages of chemisorption of oxygen on Al(100). Peaks in the projected density of states (PDOS) were calculated at approximately -9.5, -7, and -3 eV relative to the Fermi level. The first two peaks (-9.5 and -7 eV) have been observed many times in photoemission studies both for polycrystalline films[4-6] and for single-crystal surfaces[7-13]; however, the third peak (-3 eV), which we predicted and attributed to essentially oxygen nonbinding orbitals, had not been unequivocally observed. We suggested that an angle-resolved and photon-energy-dependent study be performed. Very recently, Eberhardt and Kunz[12,13] have presented the results of a photoemission study using synchrotron radiation for oxygen chemisorption on Al(100). Using 32-eV photons and collecting electrons over all polar angles from 0° to 90°, and for very low exposures (2 and 10 L, 1 langmuir $=10^{-6}$ Torr sec) of oxygen they observe a clear maximum between -2 and -3 eV, which grows with increasing exposure. With this new experimental information we may now claim complete agreement between our calculated results and experiment; three peaks were predicted and now three peaks have been observed at very nearly the same energies. Moreover, Eberhardt[13] has given results for the polarization dependence of the photoemission intensities which yield information on the character of the wave functions which should be associated with each of the two peaks (-9.5 and -7 eV). He found that on going from s to p polarization the peak at lower binding energy (-7 eV) increased in intensity while that at higher binding energy (-9.5 eV) did not, which can be interpreted, in terms of a simplified atomic model, as indicating that the peak at -7 eV contains a contribution from O $2p_z$ orbitals (perpendicular to the surface), while that at -9.5 eV does not. This is precisely the conclusion which we had previously reached from our cluster calculations (see Fig. 6 of Ref. 3). Of the calculations in the literature[5,14-17] for Al + O system our calculation[3] for a 25-atom aluminum cluster with an oxygen atom in the first surface plane is the only one to yield all three peaks at the correct energies with the decomposition into components described above. Eberhardt and Kunz[12] also presented results for the Al-2p core region which lend yet further support to our calculations. We had predicted that for the initial stages of oxidation of Al(100), when the vast ma-

jority of the surface aluminum atoms are in contact with at most a single oxygen atom, one should observe a shift to higher binding energy of the Al-2p core levels for these atoms of about 1.2 eV. A similar shift for Al(111) had previously been observed experimentally; however, the available experimental results for Al(100) showed only a 2.6-eV shift which is indicative of the formation of a bulklike oxide. Eberhardt and Kunz, working at higher resolution (the spin-orbit splitting of the Al 2p level is resolved) and a photon energy of 111.3 eV, have reported a clear peak for Al(100) plus oxygen at about 1.4 eV higher binding energy than the unperturbed Al-2p signal. A similar peak was also observed for Al(110) so it now appears that at low oxygen exposure all three low-index surfaces (100), (110), and (111) pass through an intermediate chemisorptive state before bulklike oxidation sets in.

New experimental information on the oxidation of single-crystal surfaces of aluminum is being obtained at a rapid rate in several laboratories, and we will now briefly review recent developments. It is now clear that many properties are significantly dependent on which crystal surface is exposed so that results for polycrystalline samples are of limited value as far as determining the details of the oxidation process is concerned, and so we will limit the discussion to work on single crystals.

The present theoretical study and much of the experimental work are aimed at obtaining information on (i) the geometric and (ii) the electronic structure of the Al+O system. These two goals are of course interrelated, and indeed experiments which probe the electronic structure can be used to deduce geometrical information if they are coupled with reliable geometry-dependent theoretical results. The earliest results concerning the surface structure of clean and oxygen-exposed Al(111) which are relevant to the present discussion are the low-energy electron-diffraction (LEED) results of Jona,[18] which indicated that the clean (111) surface was unreconstructed. Upon exposure to oxygen, the LEED pattern was observed to deteriorate slowly and progressively, and this was interpreted as being due to the formation of an amorphous oxide layer. However, very recently Flodström *et al.*[10] observed for 150-L exposure of Al(111) to oxygen, which corresponds approximately to a monolayer, a LEED pattern of the same symmetry as that of the clean surface but with different intensity versus voltage characteristics, and interpreted this as evidence for an ordered oxygen overlayer on a nonreconstructed surface. They also suggested that at this stage (i.e., one monolayer) the oxygen atoms are in the threefold centered site with no aluminum atom directly below (i.e., in the second layer) and at a perpendicular distance between 50 and 90 pm outside the first surface layer of aluminum atoms. It is worthwhile pointing out at this stage that the surface structure in a chemisorption system is a dynamic quantity, and indeed there may be some evidence as we will outline below, for quite significant coverage dependence of the structure for Al(111)+O. Thus, when speaking about "the structure" of the Al+O system care must be taken to specify the precise experimental conditions.

An important set of experiments on the work function of clean and oxygen-exposed low-index faces of aluminum has been performed by Gartland and co-workers,[19,20] who also used the intensity of the Al $L_{2,3}VV$ Auger transition in order to determine the sticking probability as a function of oxygen exposure. The behavior of both of these quantities was found to be qualitatively different for the (100) and (111) surfaces. The work function for Al(111) was nearly constant for oxygen exposures up to about 30 L and then increased by somewhat more than 1 eV to reach a plateau at about 100 L. In terms of the usual simplistic surface dipole interpretation of work function changes, this behavior indicates that at low coverage the oxygen atoms, which undoubtedly carry a partial negative charge, are in the first surface layer, thus yielding a zero net dipole moment perpendicular to the surface. At higher coverages (say, a monolayer) the positive shift of the work function is consistent with the oxygen atoms being outside the surface, in agreement with the suggestion of Flodström *et al.*[10] mentioned above. A kinetic analysis of the Auger data indicated that at low coverage each oxygen adsorbed removed an adsorption site so that dissolution into the bulk region must be minimal. Similar kinetics have been obtained by Martinsson *et al.*[7]

Very recently Hofmann *et al.*[21] have measured the work function for oxygen-exposed (100), (110), and (111) aluminum surfaces, using the Kelvin method rather than the photoelectric method used by Gartland *et al.*[19,20] There are significant differences between the detailed results for the two techniques, especially for the (111) surface, which have been discussed by Hofmann *et al.* However, both sets of results imply that at least two types of oxygen site are involved in the early stages of oxidation of Al(111). The first of these has the oxygen atoms incorporated in or slightly below the first surface layer, while the second which comes into play at higher exposure leads to a relative increase in the work function which implies that the oxygen atoms are outside the surface.

Further evidence that at low coverage the oxy-

gen atoms do not penetrate into the bulk region has been given by Bradshaw *et al.*[22] from an analysis of plasmon coupling to the oxygen core levels in the x-ray photoemission spectrum. They found that the surface plasmon satellite line disappeared rapidly upon oxygen exposure while the bulk plasmon line was nearly unperturbed. This was interpreted as indicating that the oxygen atoms remain outside the surface during the initial interaction. However, precise structural parameters obviously cannot be deduced from these measurements and, in particular, a model with the oxygen atoms coplanar, or nearly so, with the first surface layer of aluminum atoms cannot be ruled out.

A number of studies of Al(111)+O have been carried out by Hagström and co-workers[7-11] using a variety of techniques. Photoelectron studies using synchrotron radiation revealed peaks at about 7.1 and 9.8 eV below the Fermi level for coverages ranging from 10 to 100 L. The width of the peaks increased significantly with oxygen exposure presumably owing to increased oxygen-oxygen interactions. The part of the valence band above about −4 eV has not been carefully studied; however, as we will discuss below, further oxygen-related structure should be present in this region, similar to the case of Al(100)+O.

In this paper we present results of an extensive series of molecular-orbital calculations for clusters representing the Al(111) surface in interaction with an oxygen atom at various positions above, in, and below the surface. These calculations are aimed at providing an explanation in terms of the calculated electronic structure for these various geometrical arrangements, for the experimental data outlined above, and also to serve as a guide in the design and interpretation of future experiments. As in our previous work on Al(100)+O, the principal point of contact with experiment will be through comparison of the calculated energies and local densities of states at the oxygen atom and its surrounding aluminum neighbors with photoemission data for the valence and Al-2*p* core levels. Such comparisons can yield geometric information, albeit in an indirect fashion. Structural arrangements which yield results in marked disagreement with experiment can be safely ruled out once confidence in the theoretical method is established. In the present case such confidence is built on (i) near convergence of the clean cluster results (bandwidth and general form of the density of states) to the bulk limit, (ii) previous success of the same method and procedure for a similar study of the oxidation of Al(100), and (iii) the good agreement found with the experimental data for reasonable choices of the position of the oxygen atom.

One new aspect of the present study is that for the first time in the theoretical study of chemisorption on a metal, consideration has been given to the possibility of surface reconstruction on chemisorption. Thus two calculations have been made for large clusters (19 and 22 Al atoms) in which the central threefold site is enlarged in order to allow longer Al–O bonds for an oxygen atom in the first surface plane. As we argue in Sec. II, such a structure is consistent with all available experimental information for the earliest stages of oxygen exposure.

II. MODELS, METHOD, AND PARAMETERS

The cluster models that we have chosen to represent the (111) surface of aluminum are depicted schematically in Fig. 1. All of the clusters considered have threefold symmetry about the z axis, and oxygen chemisorption was considered only on this axis in order to maintain the symmetry (point group D_{3h} or C_{3v}). For Al(111) there are two distinct threefold sites. That depicted in Fig. 1(a) has no atom on the z axis in the second layer and we will denote this situation by a superscript (A), e.g., the 19-atom cluster shown in the figure is denoted $Al_{19}^{(A)}$. The other threefold site has an atom on the z axis in the second layer and is denoted by a superscript (B). The atomic coordinates for the largest cluster considered in each series, $Al_{19}^{(A)}$ and $Al_{22}^{(B)}$, are given in Table I. In

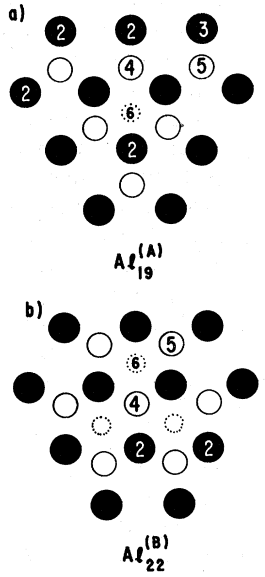

FIG. 1. View of (a) the $Al_{19}^{(A)}$ cluster and (b) the $Al_{22}^{(B)}$ cluster parallel to the (x,y) plane. The solid circles indicate atoms at $Z=0.0$, the open circles, atoms at $Z=-4.4130$ bohrs, and the dotted circles atoms at -8.8260 bohrs. Coordinates are given in Table I.

TABLE I. Atomic coordinates (bohrs, 1 bohr = 52.9177 pm) of one atom of a symmetrically related group, number of equivalent atoms in group (N), and coordination numbers (nn) for clusters of 19 ($Al_{19}^{(A)}$) and 22 ($Al_{22}^{(B)}$) aluminum atoms. The remaining coordinates can be generated by symmetry operations.

	Atom	x	y	z	N	nn
$Al_{19}^{(A)}$	Al 1	−2.7024	−1.5602	0.0	3	9
	Al 2	0.0	−6.2409	0.0	3	5
	Al 3	−5.4048	−6.2409	0.0	6	4
	Al 4	0.0	−3.1204	−4.4130	3	8
	Al 5	0.0	6.2409	−4.4130	3	5
	Al 6	0.0	0.0	−8.8260	1	3
$Al_{22}^{(B)}$	Al 1	−2.7024	−1.5602	0.0	3	9
	Al 2	0.0	−6.2409	0.0	3	6
	Al 3	−5.4048	−6.2409	0.0	6	4
	Al 4	0.0	0.0	−4.4130	1	12
	Al 5	−2.7024	−4.6807	−4.4130	6	7
	Al 6	−2.7024	1.5602	−8.8260	3	5

each case these clusters contain at least the nearest neighbors of an adsorbate placed at the origin and the nearest neighbors of these aluminum atoms. In addition to these atoms, the $Al_{19}^{(A)}$ cluster contains a further atom Al 6 in the third layer which is directly visible to the origin and so it was felt prudent to include it. These clusters are equivalent in the above sense to the Al_{25} cluster, which we found satisfactory for the (100) surface. In order to investigate the convergence of the results towards those of the bulk or the semi-infinite solid as these clusters are built up, we have performed calculations in the A series for clusters of 3 (atoms 1), 6 (atoms 1 and 2), 9 (atoms 1, 2, and 4), 12 (atoms 1, 2, and 3), 18 (atoms 1–5), and 19 atoms, and in the B series additional calculations for clusters of 19 (atoms 1–5) and 22 atoms. (See Fig. 1 for types of atoms.) For each of these clusters, calculations were performed for oxygen chemisorption by placing an oxygen atom at $Z_0 = 0.0$ and at $Z_0 = 2.0$ bohrs. For $Al_{19}^{(A)}$ and $Al_{22}^{(B)}$ additional calculations were performed for $Z_0 = 1.0$ bohr and for negative values of Z_0 corresponding to the center of the octahedral interstice for $Al_{19}^{(A)}$ ($Z_0 = -2.2065$ bohr) and the center of the tetrahedral interstice for $Al_{22}^{(B)}$ ($Z_0 = -1.1033$ bohrs). In order to examine the effect of a possible reconstruction of the surface upon oxygen adsorption, two additional calculations were carried out for $Al_{19}^{(A)}$+O and $Al_{22}^{(B)}$+O with $Z_0 = 0.0$, in which the triangle formed by the three nearest-neighbor aluminum atoms was arbitrarily expanded by 10%, leaving the other aluminum atoms in their previous unrelaxed positions. We will refer to these relaxed clusters as $Al_{19}^{(AE)}$ and $Al_{22}^{(BE)}$.

The calculations were performed with the self-consistent-field $X\alpha$ scattered-wave molecular-orbital (SCF-$X\alpha$-SW-MO) method which is well documented elsewhere.[23–25] The aluminum sphere sizes were chosen as $\frac{1}{2}$ the bulk Al-Al distance, as in our previous work. For the oxygen sphere, a radius of 1.12 bohrs was used for all cases in order to avoid unreasonably small values which would result if one used tangent muffin-tin spheres. This corresponds to the radius of a sphere which will just fit in the octahedral interstice of close-packed aluminum atoms. Most of the calculations, therefore, involve nonzero overlap of the aluminum and oxygen spheres. Our previous study of Al(100)+O indicated that the properties of interest are quite insensitive to reasonable variations in the radius of the oxygen sphere. As in our previous work, in the solution of the secular equations, partial waves up to $l = 1$ were included for Al and O and up to $l = 2$ in the extramolecular region. The exchange parameters were taken from the compilation of Schwarz[26] and have the value $\alpha = 0.728\,53$ for aluminum and $\alpha = 0.744\,47$ for oxygen. In the intersphere and extramolecular regions the aluminum value was used.

III. RESULTS AND DISCUSSION

In a cluster study which purports to model an infinite or semi-infinite solid it is important to ensure that a sufficient number of atoms have been included to yield converged results for the property of interest. The convergence of the present series of calculations is illustrated in Fig. 2, which shows

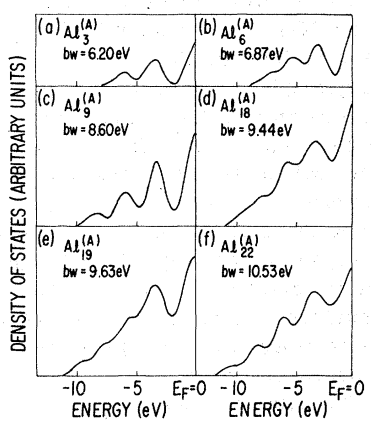

FIG. 2. Density of states (arbitrary units) of the occupied valence band for representative clusters of various sizes vs orbital energy (eV) relative to the Fermi level. The curves were generated by replacing each discrete cluster eigenvalue by a Gaussian of width parameter 0.68 eV. bw is the width (in eV) of the occupied valence band.

the density of states (DOS) of the occupied valence band for some representative clusters. The curves were generated by replacing each discrete energy level by a Gaussian of width parameter 0.05 Ry and then summing the Gaussians point by point. Also shown for each cluster is the value of *bw*, the occupied valence bandwidth. The curves are very similar to those previously presented[3] for clusters of similar numbers of atoms, representing the (100) surface. The smaller clusters have a bandwidth which is far too small and also large gaps in the DOS. As more atoms are added the bandwidth increases and the gaps fill in. The largest member of each series has a DOS which is similar in all important respects to that previously found for the Al_{25} cluster of C_{4v} symmetry, which was succesfully used to represent Al(100). In particular, the bandwidth is calculated to be 9.6 eV for $Al_{19}^{(A)}$ and 10.5 eV for $Al_{22}^{(B)}$, which represent, respectively, 85% and 93% of the bulk bandwidth deduced from x-ray studies.[27] The DOS for the larger clusters is approximately free-electron-like with, however, significant structure particularly in the region between −5 eV and the Fermi level, as discussed previously.[2] Thus we conclude that $Al_{19}^{(A)}$ and $Al_{22}^{(B)}$ are likely to be reasonably converged models of the (111) surface for our purposes. The smaller clusters would be less reliable and indeed examination of the projected DOS (PDOS) curves for the oxygen atom (see below) shows significant qualitative differences between clusters containing less than 18 atoms and $Al_{19}^{(A)}$ or $Al_{22}^{(B)}$. This is illustrated in Fig. 3, where we compare the PDOS curve for oxygen at $Z_0 = 2.0$ bohrs for a 9-atom cluster $Al_9^{(A)}$, atom types 1, 2, and 4) with the corresponding curve for $Al_{19}^{(A)}$ +O. These curves were generated in a similar fashion to the DOS curves except that the Gaussians were weighted with the calculated charge inside the oxygen sphere. A cursory examination of Fig. 3 is sufficient to show that the two clusters yield quite different results. In the remainder of this paper we will therefore consider only the two largest clusters.

We will now consider the interaction of $Al_{19}^{(A)}$ and $Al_{22}^{(B)}$ with an oxygen atom placed at various positions on the z axis. For the moment only the unrelaxed surface will be considered; we will consider the possibility of surface relaxation below. The (111) surface is significantly more densely packed than the (100) surface previously considered. This is illustrated in Fig. 4, which shows the geometrical arrangement of the two surfaces side by side. The small circle in each case represents a sphere which will just fit in the octahedral interstice. As a point of comparison, the two situations shown correspond, for $Z_0 = 0.0$, to

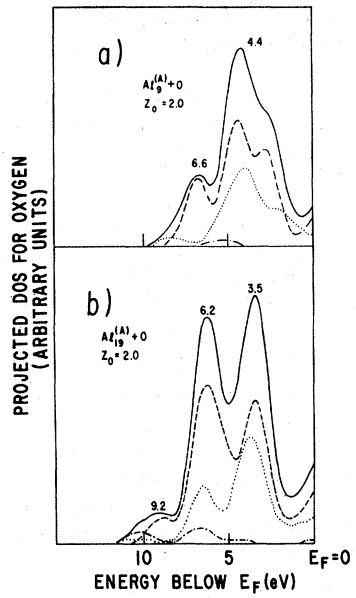

FIG. 3. Comparison of the projected density of states for the oxygen atom vs orbital energy (eV relative to Fermi level) for aluminum clusters interacting with an oxygen atom at $Z_0 = 2.0$ bohrs. (a) $Al_9^{(A)}$+O (b) $Al_{19}^{(A)}$+O; solid lines, total PDOS, dashed lines, contribution from p_x and p_y orbitals; dotted lines, contribution from p_z dot-dashed lines, contribution from s orbitals.

Al–O bond lengths of 202 and 165 pm, respectively, for Al(100) and Al(111), which may be compared with the Al–O bond length of 197 pm for the oxide Al_2O_3. The interlayer spacing is also quite different for the two surfaces being 202 pm for Al(100) and 234 pm for Al(111). Thus one might expect that for the same value of Z_0 the electronic structure of the Al +O system would be quite different for the two surfaces which is in fact the case as we discuss below.

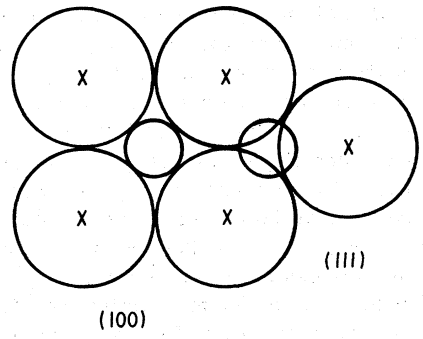

FIG. 4. Comparison of the geometries of ideal (100) and (111) surfaces of a face-centered-cubic crystal. The four leftmost large circles represent a (100) surface while the three rightmost large circles represent a (111) surface. The smaller circles are of the appropriate size to fit exactly into an octahedral interstice.

For the valence region, our results are presented in Fig. 5 in the form of PDOS curves. The curves have also been decomposed into components due to s, p_z (perpendicular to the surface, representation a_1 of C_{3v}) and the sum of p_x and p_y (parallel to the surface, representation e of C_{3v}) partial waves in order to help characterize the bonding.

For each type of site, (A) and (B), results are shown for the oxygen atom in the interstice [octahedral for (A), tetrahedral for (B)] immediately below the central threefold site; for the oxygen in the first surface plane, $Z_0 = 0.0$ and for two distances, $Z_0 = 1.0$ bohr and $Z_0 = 2.0$ bohrs above the surface. If one accepts that these models are converged and that the computational method is sufficiently accurate as indicated by its success for Al(100)+O, then Fig. 5 can be used to deduce geometrical information by comparison with experimental photoemission data. For the present case, peaks have been observed at about −7.1 and −9.8 eV for a wide range of oxygen exposure. The form of the experimental photoemission bands are quite reminiscent of those for Al(100)+O, with the structure at −7.1 eV being significantly more intense. The region above −5 eV has not been discussed; however, all of the curves in Fig. 5 show significant oxygen-related structure in this region which is due to essentially nonbonding orbitals (see below). We are confident that this structure will eventually be observed experimentally, as it was for Al(100)+O subsequent to our calculations. Using the two peaks at −7.1 and −9.8 eV as criteria we may now examine the curves of Fig. 5 to see which oxygen position, if any, is consistent with these data.

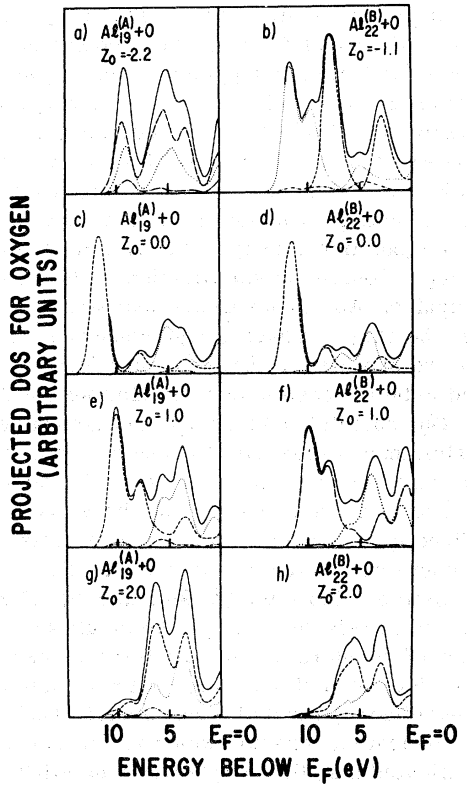

FIG. 5. Projected density of states for the oxygen atom vs orbital energy (eV relative to Fermi level) for aluminum clusters interacting with an oxygen atom at various positions; (a) $Al_{19}^{(A)}$+O, $Z_0 = -2.2$ bohrs; (b) $Al_{22}^{(B)}$+O, $Z_0 = -1.1$ bohrs; (c) $Al_{19}^{(A)}$+O, $Z_0 = 0.0$; (d) $Al_{22}^{(B)}$+O, $Z_0 = 0.0$; (e) $Al_{19}^{(A)}$+O, $Z_0 = 1.0$ bohrs; (f) $Al_{22}^{(B)}$+O, $Z_0 = 1.0$ bohrs (g) $Al_{19}^{(A)}$+O, $Z_0 = 2.0$ bohrs; (h) $Al_{22}^{(B)}$+O, $Z_0 = 2.0$ bohrs. See Fig. 3 for symbols.

First, for negative values of Z_0, Figs. 5(a) and 5(b), the PDOS curves bear little resemblance to experiment. For oxygen in the octahedral interstice [Fig. 5(a)] there is no peak near −7 eV, while for the tetrahedral interstice [Fig. 5(b)] an intense peak is predicted at −11.6 eV, while no such peak has been observed experimentally. Thus our calculations add further evidence to the experimental conclusion mentioned in the Introduction that the oxygen atoms do not lie below the first layer of aluminum atoms during the initial stages of oxidation. Figures 5(c) and 5(d) show the results for $Z_0 = 0.0$, i.e., the oxygen atom in the unrelaxed first surface plane. This position of the oxygen would be consistent with a constant work function during the initial stages of chemisorption and also with the kinetics results, since an oxygen atom at $Z_0 = 0.0$ (or any positive value) clearly eliminates an adsorption site. The PDOS curves, however, indicate that for this geometry the dominant feature of the spectrum should be a peak at −11.4 eV due to in-plane p orbitals of the oxygen. No such peak has been observed for exposures as low as 10 L (where the work function still has very nearly its clean-surface value). We therefore conclude that the oxygen cannot be at $Z_0 = 0.0$ for an unrelaxed surface.

Figures 5(e) and 5(f) show the results for $Z_0 = 1.0$ bohr, which now are clearly starting to resemble the experimental spectrum. For the (A) site, peaks are calculated at −10.0 and −7.6 eV, while for the (B) site the values are −9.6 and −7.8 eV. Both of these peaks are due to orbitals which are parallel to the surface. The features due to p_z (perpendicular) orbitals are found only at lower binding energies giving rise to peaks at −5.4, −3.5, and −0.5 eV for the (A) site and at −5.9, −3.5, and −0.5 eV for the (B) site. Thus having the oxygen near $Z_0 = 1.0$ seems to be at least an improvement over the previously discussed positions. However, there are two features of the PDOS curves which indicate that $Z_0 = 1.0$ is not the exact position. First, the relative inten-

sities of the PDOS peak at about −10 and −7.6 eV are reversed with respect to experiment. Of course such a comparison is not rigorously justified because of the possibility of matrix element effects; however, our past experience with Al(100)+O was that for similar orbitals at similar energies the relative intensities were calculated to be qualitatively correct. Second, both of the calculated curves at $Z_0 = 1.0$ bohr have a peak near −5.5 eV which has not been observed.

If one follows the evolution of the peaks due to parallel p orbitals on going from $Z_0 = 0.0$ to $Z_0 = 1.0$ [compare Fig. 5(c) to 5(e) or Fig. 5(d) to Fig. 5(f)], one observes a shift of the highest-binding-energy peak to lower binding energies [−11.4 to −10.0 eV for the (A) site, −11.4 to −9.6 eV for the (B) site] and at the same time an increase in intensity of the peak near −7.5 eV. Thus further increase of the oxygen-surface distance should tend to bring the PDOS into better agreement with experiment.

The results for $Z_0 = 2.0$ bohrs are shown in Fig. 5(g) for the (A) site and Fig. 5(h) for the (B) site. The above trend is indeed evident, although it is somewhat exaggerated, indicating that $Z_0 = 2.0$ bohrs is somewhat too far out for the oxygen. For the (A) site the calculations gives peaks at −3.5, −6.2, and −9.2 eV, the last being quite weak compared with that at −6.2 eV. For the (B) site, peaks are found at −2.6 and −5.5 eV with a weak shoulder at about −9 eV. Thus for $Z_0 = 2.0$ bohrs, the relative intensities of the various peaks are in better agreement with experiment than for $Z_0 = 1.0$ but the energies of the peaks are somewhat worse. It is clear on examining the trends in the various peaks and their components as a function of Z_0 that at some distance between $Z_0 = 1.0$ and 2.0 bohrs, agreement between the calculations and experiment will be found within the accuracy limits of both. A value of $Z_0 = 2.03$ bohrs would yield an Al–O distance of 197 pm, which is the Al–O bond distance in Al_2O_3 so that the above position range seems reasonable. This geometry is also consistent with all available experimental evidence with the possible exception of the work-function data for low coverage, which imply a value near $Z_0 = 0.0$ if they are interpreted in terms of the surface dipole model. The latter model is of course highly simplistic and so the geometrical interferences are far from being unequivocal.

For $Z_0 = 2.0$ bohrs, the PDOS for $Al_{19}^{(A)}$+O and indeed its decomposition into components are quite similar to what we found for Al(100)+O using a 25-atom cluster and placing the oxygen at $Z_0 = 0.0$. The highest-binding-energy peak at −9.2 eV for $Al_{19}^{(A)}$+O is primarily due to p_x and p_y orbitals; the peaks at −6.2 and −3.5 eV receive significant contributions from both types of p orbitals. Measurement of the polarization dependence of the photoemission for this surface similar to those made for Al(100)+O by Eberhardt[13] would be highly desirable in order to verify this aspect of our calculations. In order to better characterize the peaks we have generated contour plots of the relevant wave functions which reveal that again, similar to the case of Al(100)+O mentioned above, the two highest-binding-energy peaks correspond to orbitals which are bonding between the aluminum and oxygen atoms, whereas the orbitals which contribute to the peak at −3.5 eV are best classified as nonbonding. Four representative contour plots are presented in Fig. 6 in order to illustrate this point. Figures 6(a) and 6(b) show orbitals of e symmetry plotted in a plane through the oxygen, parallel to the surface. The orbital at −6.7 eV [Fig. 6(a)] has a significant bonding interaction between the oxygen and the aluminums, while very little interaction is present for the nonbonding e orbital at −3.7 eV [Fig. 6(b)]. Similar comments apply for the orbitals of a_1 symmetry which are plotted in the yz plane in Figs. 6(c) and 6(d).

Further confirmation for a value of Z_0 in the vicinity of 2 bohrs for the unrelaxed surface may be obtained from a comparison of the Al-2p photoemission results[10] with our calculations. Experimentally, the first stages of oxidation yield a shift of the Al-2p line to higher binding energy by about 1.4 eV. Such shifts are usually interpreted in terms of charge transfer from aluminum to oxygen, the positive charge on the aluminum atom causing a Coulombic stabilization of the Al-2p eigenvalue. As the adsorbate approaches the surface, the charge transfer, and consequently, the shift are expected to increase, and indeed this was found to be the case in our calculations for Al(100)+O. Our calculated Al-2p orbital eigenvalues for the aluminum atoms (Al 1) adjacent to the oxygen in the first surface layer are shown in Table II. These are unrelaxed values and therefore may not be directly compared with the experimental ionization energies; however, all of the levels are of very similar character (Al 2p), and therefore any differential relaxation should be small so that the values of the shifts (Δ is the difference between ϵ_{2p} for the clean cluster and for the oxygen containing cluster) should be meaningful. Our calculations indicate a behavior which is somewhat more complicated than the simple Coulomb effect mentioned above. For the shortest Al-O distances considered ($Z_0 = 0.0$) we actually calculate a net destabilization of the Al 2p level. This is, at first sight, surprising; however, it must be remembered that in this geometrical situation any electrons transferred to the oxygen are not too far removed from the aluminum and so, in a strictly Coulombic

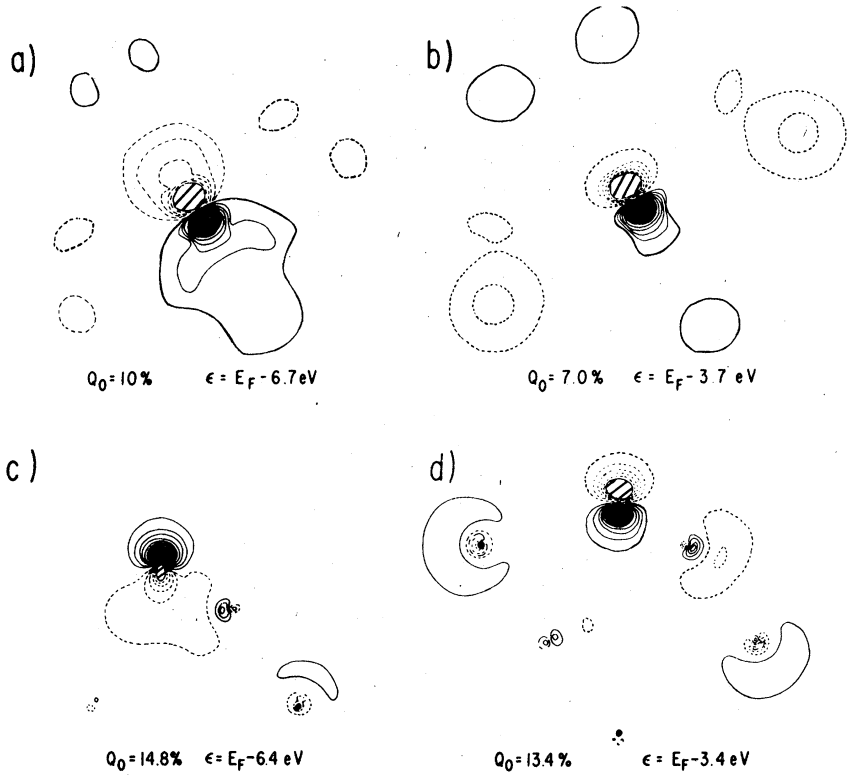

FIG. 6. Contour maps of selected molecular-orbital wave functions for $Al_{19}^{(A)}$ + O, $Z_0 = 2.0$ bohrs. (a) and (b) show orbitals of e symmetry plotted in a plane through the oxygen, parallel to the surface; (c) and (d) show orbitals of a_1 symmetry plotted in the (y,z) plane [perpendicular to the surface (see Table I)]. The solid (positive) and hatched (negative), regions near the oxygen atom represent regions of many closely spaced contours. Solid lines indicate positive value of wave functions. Dashed lines indicate negative value of wave functions. The levels shown are at (a) -6.7, (b) -3.7, (c) -6.4, and (d) -3.4 eV with respect to the Fermi level and correspond to percentage charges within the oxygen sphere of (a) 10.2%, (b) 7.0%, (c) 14.8%, and (d) 13.4%.

picture, the destabilizing field of the oxygen would have to be considered as well as the stabilizing field of the positively charged aluminum. As the Al-O distance increases, the calculated shift also increases and attains a value somewhat greater than +1 eV for $Z_0 = 2.0$ bohrs (and also for the octahedral interstice of $Al_{19}^{(A)}$ +O; however, this position has been ruled out on the basis of the valence photoemission data). Thus for a value of Z_0 near 2.0 bohrs one finds agreement with experiment, adding further evidence for the possibility of this position for the chemisorbed oxygen atom.

As we saw above, if the oxygen atom is placed at $Z_0 = 0.0$ for an unrelaxed cluster, the resultant PDOS curve is not consistent with the photoemission data. This is not too surprising if one compares the Al-O distance involved, 165 pm, with that for a "normal" Al-O bond, about 197 pm. We have therefore examined the effects of a possible local expansion of the surface which increases the size of the threefold site. For the $Al_{19}^{(AE)}$ +O and $Al_{22}^{(BE)}$ +O clusters we have arbitrarily expanded by 10% the triangle formed by the three central aluminum atoms. This yields an Al-O distance of 182 pm. The PDOS curves for these two calculations are shown in Fig. 7.

It is clear from a comparison of Fig. 7(a) with Fig. 5(c) or Fig. 7(b) with Fig. 5(d) that a 10% ex-

TABLE II. Orbital eigenvalues ϵ_{2p} (Rydbergs) for the Al-2p derived levels of Al 1 for 19- and 22-atom aluminum clusters interacting with an oxygen atom. Δ is the shift in eV with respect to the corresponding clean-cluster result.

	$Z_0 = 2.0$			$Z_0 = 1.0$		$Z_0 = 0.0$		$Z_0 = -1.1$		$Z_0 = -2.2$	
	$-\epsilon_{2p}$	$-\epsilon_{2p}$	Δ	$-\epsilon_{2p}$	Δ	$-\epsilon_{2p}$	Δ	$-\epsilon_{2p}$	Δ	$-\epsilon_{2p}$	Δ
$Al_{19}^{(A)}$	5.422	5.507	1.16	5.456	0.46	5.419	−0.04			5.505	1.13
$Al_{22}^{(B)}$	5.494	5.575	1.10	5.517	0.31	5.475	−0.26	5.504	0.14		
$Al_{19}^{(AE)}$	5.419					5.471	0.71				
$Al_{22}^{(BE)}$	5.488					5.580	1.25				

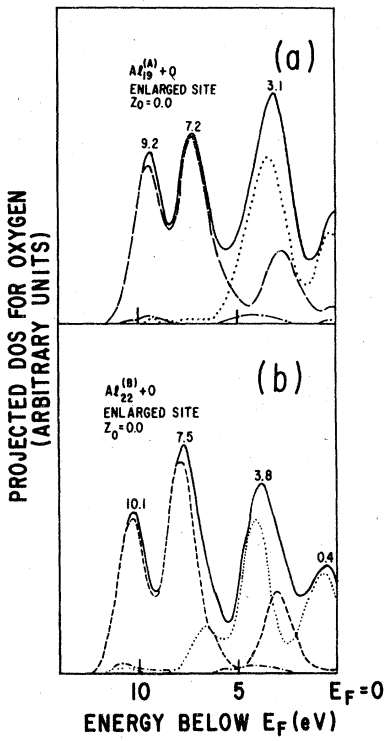

FIG. 7. Projected density of states for the oxygen atom vs orbital energy (eV relative to Fermi level) for (a) the $Al_{19}^{(AE)}$ and (b) $Al_{22}^{(BE)}$ cluster interacting with an oxygen atom at $Z_0=0.0$. For these clusters the triangle formed by the three central aluminum atoms has been expanded by 10%. See Fig. 3 for symbols.

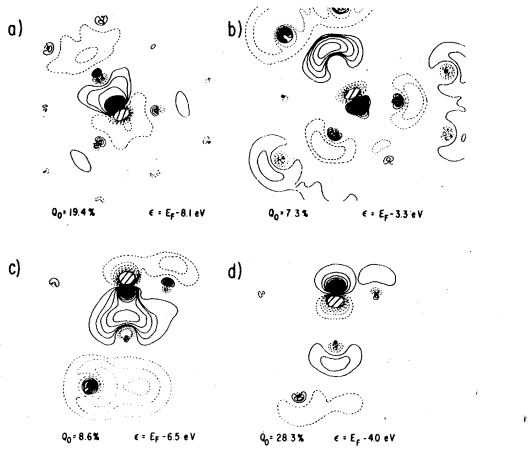

FIG. 8. Contour maps of selected molecular-orbital wave functions for $Al_{22}^{(BE)}$+O, $Z_0=0.0$. (a) and (b) show orbitals of e symmetry plotted in the surface plane (x,y); (c) and (d) show orbitals of a_1 symmetry plotted perpendicular to the surface [(y,z) plane] (see Table I). The levels shown are at (a) -8.1, (b) -3.3, (c) -6.5, and (d) -4.0 eV with respect to the Fermi level and correspond to percentage charges within the oxygen sphere of (a) 19.4%, (b) 7.3%, (c) 8.6%, and (d) 28.3%. See Fig. 6 for symbols.

pansion has a drastic effect on the electronic structure. Both of the expanded clusters give results which are in quite reasonable agreement with the experimental photoemission data, $Al_{19}^{(AE)}$+O having peaks at -7.2 and -9.2 eV and $Al_{22}^{(BE)}$+O having peaks at -7.5 and -10.1 eV, all with reasonable relative intensities. In both cases, both of these peaks are primarily due to p orbitals parallel to the surface. Indeed the only qualitative difference between the two types of site is a small peak due to p_z orbitals near -6.7 eV for $Al_{22}^{(BE)}$+O. This cluster has an aluminum atom directly below the oxygen in the second layer and so some bonding interaction is present. Further structure is again found between -5 eV and the Fermi level. Once again, analysis of the wave functions shows that the peaks near -9.5 and -7.5 eV are due to Al-O bonding orbitals while that near -3.5 eV is due to essentially nonbonding oxygen p orbitals. Figure 8 shows four representative contour plots for $Al_{22}^{(BE)}$+O. Similar orbitals exist for $Al_{19}^{(BE)}$+O with the exception of that shown in Fig. 8(c), which involves σ bonding between the oxygen and the aluminum atom directly below in the second layer. This latter atom is not present in the $Al_{19}^{(A)}$ cluster, and therefore such interactions are not possible. While the presence of this orbital for the (B) site and its absence for the (A) site does not lead to any qualitative difference in the PDOS at this level of resolution, it might in the future prove possible to detect its presence or absence by studying the photon energy, polarization, and angle dependence of the photoemission intensity and thereby, to distinguish between the two possible sites, if indeed, at some oxygen exposure, the geometry is similar to that considered here.

Finally, we note that expanding the threefold site for $Z_0=0.0$ causes the Al $2p$ levels (see Table II) to shift in the direction observed experimentally. The calculated shifts of 0.71 eV for $Al_{19}^{(AE)}$+O and 1.25 eV for $Al_{22}^{(BE)}$+O are in adequate agreement with the experimentally observed shift of 1.4 eV, especially considering the arbitrariness of the extent of expansion. This leads to the conclusion that a locally expanded surface with $Z_0=0$ is compatible with the experimental data.

Thus it appears from the above discussion that at the current level of sophistication of both experimental and theoretical methods one is unable to distinguish unequivocally between two possible structural models for the initial stages of oxidation of Al(111). The first has the oxygen outside an unreconstructed surface, in the vicinity of Z_0 =2.0 bohrs, while the second has the oxygen in

the first surface layer ($Z_0 = 0.0$) of a locally expanded surface. The arrangement with the oxygens outside the surface has the appeal of simplicity, since an ordered overlayer can be formed without disturbing the arrangement of the metal atoms. It would, however, lead to a quite complicated explanation of the work function changes; in particular, an explanation of the increase near 30 L, which is still below a monolayer coverage, would probably require the consideration of adsorbate-adsorbate interactions if the individual oxygen atoms maintain their low-coverage positions. On the other hand, the low-coverage model with oxygen atoms in a locally expanded surface leads to a simple explanation of the work-function data, but requires a more dynamic view of the oxidation process. In this model, at low coverage the oxygens are in a relaxed surface at $Z_0 = 0.0$; as the coverage increases the surface becomes, at a certain point (probably near $\frac{1}{6}$ of a monolayer), unable to accomodate further local expansions, and the oxygens take up positions outside the surface, the aluminum atoms returning to their previous positions to eventually yield an ordered monolayer situation. Clearly, more work is required to establish whether either of these pictures is valid. All we can say for the moment is that both are reasonable working hypotheses.

IV. CONCLUSION

The calculations described above have yielded information on the electronic structures of large-cluster models for the system Al(111) + O, which give every indication of being sufficiently converged to the infinite limit for the purposes for which they were used. These results, coupled with the available experimental photoemission data, suggest two distinct possible local geometries for the Al + O complex, both of which may in fact be present at various stages of the initial oxidation of Al(111). For each of the two structural arrangements, peaks in the projected density of states for the oxygen atom are calculated at energies in good agreement with those of the observed oxygen-induced structure in the photoemission experiments for a wide range of oxygen exposure. Analysis of the cluster wave functions suggests, however, that significant differences exist between the two cases in the character of the orbitals responsible for the peaks. These differences should be detectable by varying the incident light polarization and/or the angular variables in the experiments. A systematic study of this type, as a function of several experimental parameters such as the oxygen exposure, the pressure at which the experiments are performed, the temperature, etc., coupled with our calculated results or future similar calculations as the need arises, afford the exciting possibility of using photoemission data to monitor the structural parameters as oxidation takes place.

It is becoming more and more clear that Al + O is not the well-behaved model system it was once hoped to be and that much more work, both experimental and theoretical, will be needed before a true understanding of the details of the chemisorption of oxygen on aluminum and the subsequent development of aluminum oxide will be obtained. Nevertheless, the present calculations for Al(111) + O and our previous calculations for Al(100) + O have provided much insight into a number of aspects of the aluminum-oxygen interaction for these two surfaces. Similar studies are now in progress for the third important low-index surface Al(110).

ACKNOWLEDGMENTS

Financial support (to D. R. S.) from the National Research Council of Canada is gratefully acknowledged. We are grateful to C. Kunz, W. Eberhardt, and A. M. Bradshaw for the communication of results prior to publication.

[1] R. P. Messmer and D. R. Salahub, Chem. Phys. Lett. 49, 59 (1977).
[2] D. R. Salahub and R. P. Messmer, Phys. Rev. B 16, 2526 (1977).
[3] R. P. Messmer and D. R. Salahub, Phys. Rev. B 16, 3415 (1977).
[4] S. A. Flodström, L. -G. Petersson, and S. B. M. Hagström, J. Vac. Sci. Technol. 13, 280 (1976).
[5] K. Y. Yu, J. N. Miller, P. Chye, W. E. Spicer, N. D. Lang, and A. R. Williams, Phys. Rev. B 14, 1446 (1976).
[6] S. A. Flodström, L. -G. Petersson, and S. B. M. Hagström, Solid State Commun. 19, 257 (1976).
[7] C. Martinsson, L. -G. Petersson, S. A. Flodström, and S. B. M. Hagström, in Proceedings of the International Study Conference on Photoemission from Surfaces, Noordwijk, Holland, 1976 (unpublished).
[8] R. A. Bachrach, S. A. Flodström, R. S. Bauer, S. B. M. Hagström, and D. J. Chadi, in Proceedings of the Seventh International Vacuum Congress and Third International Conference on Solid Surfaces, Vienna, 1977 (unpublished).
[9] S. A. Flodström, R. Z. Bachrach, R. S. Bauer, and S. B. M. Hagström, in Ref. 8.
[10] S. A. Flodström C. W. B. Martinsson, R. Z. Bachrach, S. B. M. Hagström, and R. S. Bauer, Phys. Rev. Lett. 40, 907 (1978).
[11] R. Z. Bachrach, S. A. Flodström, R. S. Bauer, S. B.

M. Hagström and D. J. Chadi, J. Vac. Sci. Technol. 15, 488 (1978).
[12]W. Eberhardt and C. Kunz, Surf. Sci. (to be published).
[13]W. Eberhardt, Ph.D. thesis (Universität Hamburg, 1978) (unpublished).
[14]N. D. Lang and A. R. Williams, Phys. Rev. Lett. 34, 531 (1975).
[15]J. Harris and G. S. Painter, Phys. Rev. Lett. 36, 151 (1976).
[16]I. P. Batra and S. Ciraci, Phys. Rev. Lett. 39, 774 (1977).
[17]G. S. Painter, Phys. Rev. B 17, 662 (1978).
[18]F. Jona, J. Phys. Chem. Solids 28, 2155 (1967).
[19]J. K. Grepstad, P. O. Gartland, and B. J. Slagsvold, Surf. Sci. 57, 348 (1976).
[20]P. O. Gartland, Surf. Sci. 62, 183 (1977).
[21]P. Hofmann, W. Wyrobisch, and A. M. Bradshaw, Surf. Sci. (to be published).
[22]A. M. Bradshaw, W. Domcke, and L. S. Cederbaum, Phys. Rev. B 16, 1480 (1977).
[23]J. C. Slater, Adv. Quantum Chem. 6, 1 (1972), and references therein.
[24]K. H. Johnson, Adv. Quantum Chem. 7, 143 (1973), and references therein.
[25]For recent reviews, see, e.g., K. H. Johnson, Ann. Rev. Phys. Chem. 26, 39 (1975); R. P. Messmer, in *Modern Theoretical Chemistry*, edited by G. A. Segal (Plenum, New York, 1977), Vol. 8, p. 215; N. Rösch, in *Electrons in Finite and Infinite Structures*, edited by P. Phariseau (Plenum, New York, 1977)); R. P. Messmer, in *The Nature of the Surface Chemical Bond*, edited by G. Ertl and T. N. Rhodin (North-Holland, Amsterdam, 1978).
[26]K. Schwarz, Phys. Rev. B 5, 2466 (1972).
[27]G. A. Rooke, J. Phys. C 1, 767, 776 (1968).